Scientific Research Publishing

Journal of Geographic Information System, 2026, 18(2), 107-127
https://www.scirp.org/journal/jgis
ISSN Online: 2151-1969
ISSN Print: 2151-1950

A GIS-Based Spatial Null Model Framework for Evaluating Logarithmic Spiral Patterns in Point Sets

Sam Osmanagich

Archaeological Park: Bosnian Pyramid of the Sun Foundation, Visoko, Bosnia and Herzegovina
Email: info@drsamosmanagich.com

How to cite this paper: Osmanagich, S. (2026) A GIS-Based Spatial Null Model Framework for Evaluating Logarithmic Spiral Patterns in Point Sets. *Journal of Geographic Information System*, **18**, 107-127.
https://doi.org/10.4236/jgis.2026.182006

Received: January 12, 2026
Accepted: March 14, 2026
Published: March 17, 2026

Abstract

This study develops and applies a GIS-based spatial null model framework to evaluate whether observed point sets exhibit constrained logarithmic spiral patterns beyond what would be expected under spatial randomness and alternative structured configurations. We integrate exhaustive enumeration, Monte Carlo randomization, and constraint-preserving null ensembles within a GIS environment that explicitly limits geometric degrees of freedom to test multiple candidate geometric hypotheses. Spatial datasets of summit coordinates were prepared and analyzed as standardized GIS point layers to demonstrate practical implementation. Null models preserve varying degrees of spatial constraints to reflect alternative generative processes. The framework quantifies departures from each null distribution using robust pattern statistics, emphasizing reproducibility and transferability across spatial datasets. Results highlight the approach's capacity to distinguish between random, constraint-driven, and highly structured spiral configurations in point patterns. This methodology operationalizes falsification-based spatial hypothesis testing in GIS research and offers a generalizable toolset for pattern analysis in geographic information systems.

Keywords

Spatial Null Models, GIS, Point Pattern Analysis, Logarithmic Spiral, Monte Carlo

1. Introduction

Detecting and evaluating large-scale geometric structure in spatial point data is a recurring challenge in geographic information system (GIS) research. Apparent

spatial regularities can emerge from visual perception, data sparsity, or flexible geometric fitting rather than from underlying spatial processes. As a result, claims of non-random geometric organization in geographic datasets require careful quantitative evaluation using explicitly defined constraints and null hypotheses [1] [2]

Recent advances in geospatial data acquisition, particularly high-resolution LiDAR and digital terrain models, have improved the positional accuracy of point-based representations of landscape features [3] [4]. Within a GIS framework, such datasets enable systematic analysis of spatial relationships among discrete geographic objects using methods drawn from spatial statistics, computational geometry, and spatial modeling. These tools allow hypotheses concerning spatial structure to be tested directly against alternative stochastic and constrained models rather than inferred from visual alignment alone.

Among candidate geometric forms, logarithmic spirals occupy a distinctive position (**Figures 1-7**). They appear in a range of natural and engineered systems, yet they are also highly flexible mathematical constructs (**Figure 8**). Without well-defined limits on anchoring, orientation, growth parameters, and spatial tolerance, spiral models can be adjusted to accommodate sparse or irregular point distributions. Consequently, meaningful detection of spiral-like structure in spatial data requires more than curve fitting; it requires explicit rejection criteria and comparison against appropriate null ensembles [5] [6] (**Figures 9-20**).

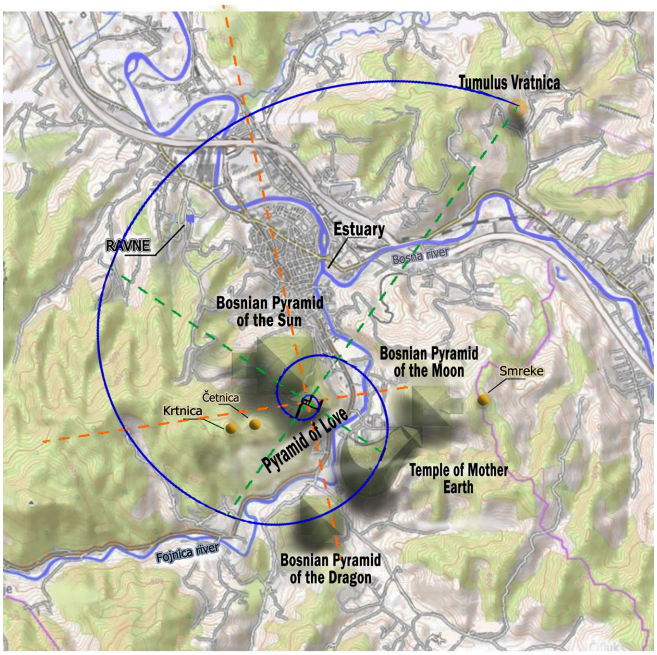

Figure 1. GIS-based representation of the tested logarithmic spiral hypothesis applied to a spatial point dataset. The spiral is defined using golden-ratio growth and evaluated against five selected summit locations represented as GIS point features in projected coordinates: Bosnian Pyramid of the Sun, Pyramid of Love, Bosnian Pyramid of the Dragon, Bosnian Pyramid of the Moon, and the Vratnica Tumulus. This figure illustrates the initial geometric hypothesis prior to statistical testing.

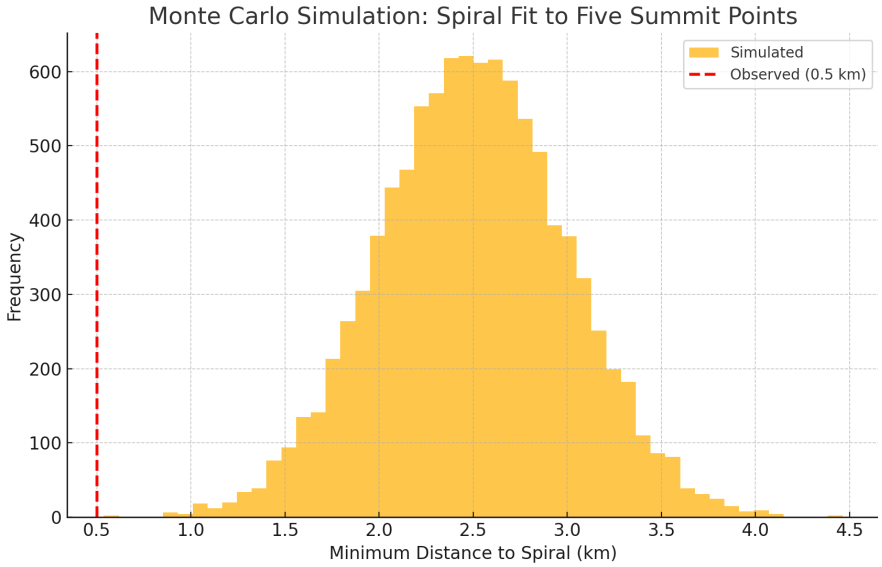

Figure 2. Results of uniform random Monte Carlo simulation under a spatial tolerance of 0.5 km. Five points are randomly generated within the study extent, and a logarithmic spiral is anchored at one point. No simulated configuration satisfies the fitting criterion.

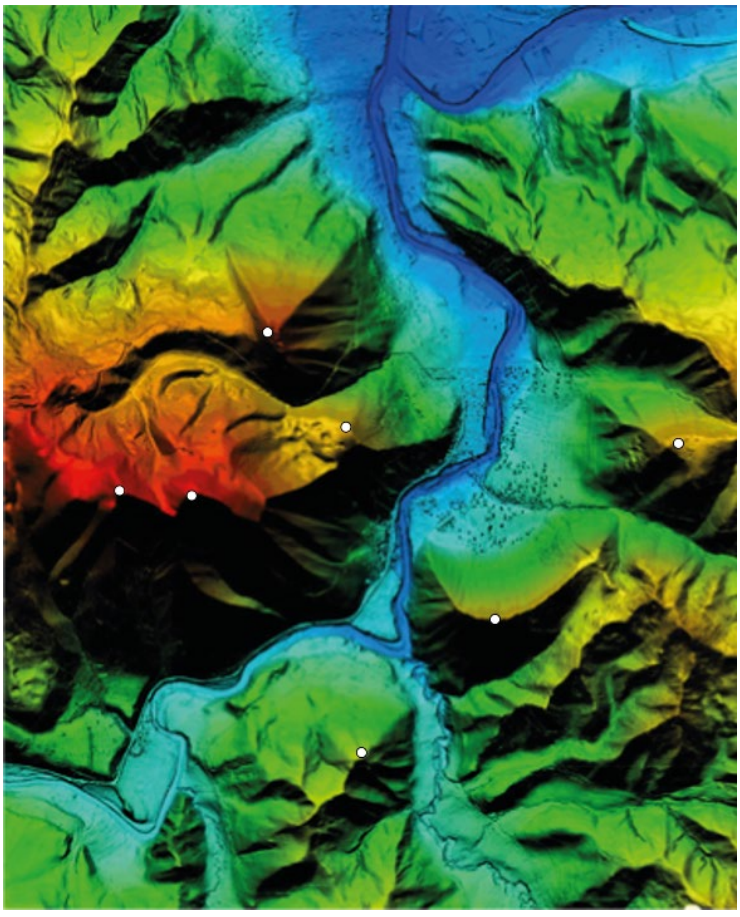

Figure 3. LiDAR-derived digital terrain model used for summit identification and coordinate extraction. Summit locations are derived from high-resolution elevation data and represented as fixed GIS point features. Positional accuracy is sub-meter.

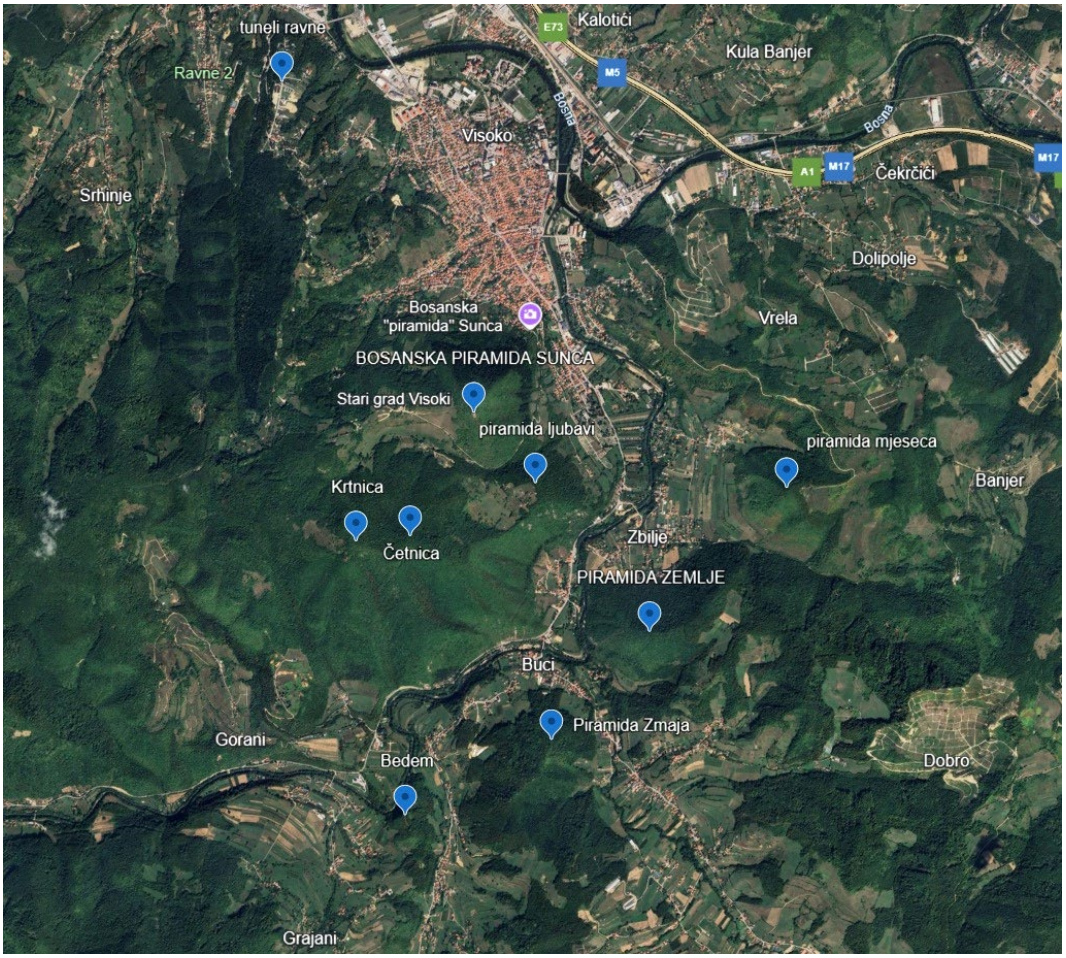

Figure 4. Spatial distribution of analyzed summit locations represented as GIS point features within the study area. Only named and cartographically documented summits are included.

Location	Latitude	Longitude	Y Gauss- Kruger	X Gauss -Kruger	apsolutna kota
Bosnian Pyramid of the Sun	43°58'36"N	18°10'35"E	6514549.010	4870258.900	764.856
Temple of Mother Earth	43°57'51"N	18°11'24"E	6515656.180	4868887.120	659.695
Tumulus in Vratnica	44°00'28"N	18°12'56"E	6517695.090	4873744.790	506.710
Bosnian Pyramid of the Moon	43°58'20"N	18°12'03"E	6516518.910	4869793.150	666.060
Tunnel Ravne Entrance	43°59'44"N	18°09'39"E	6513311.590	4872362.840	496.650
Bosnian Pyramid of Love	43°58'21"N	18°10'51"E	6514934.430	4869818.840	668.310
Bosnian Pyramid of Dragon	43°57'29"N	18°10'56"E	6515038.980	4868199.190	595.530
Krtnice	43°58'09"N	18°10'01"E	6513819.850	4869456.670	844.000
Četnice	43°58'11"N	18°10'17"E	6514157.130	4869489.700	836.340
Bedem	43°57'13"N	18°10'14"E	6514109.610	4867713.720	527.510

Figure 5. Coordinate table of analyzed summit locations. Geographic coordinates, projected Gauss-Krüger coordinates, and absolute elevations are reported. These values are treated as fixed inputs across all analyses.

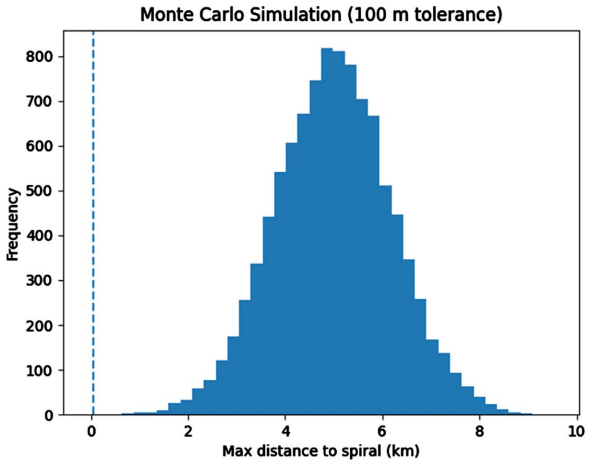

Figure 6. Uniform random Monte Carlo simulation results under a spatial tolerance of 100 m. No simulated configuration satisfies the spiral fitting criterion across 100,000 realizations.

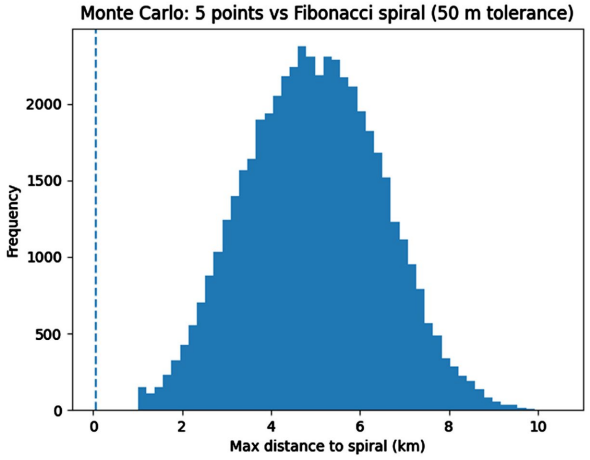

Figure 7. Uniform random Monte Carlo simulation results under a spatial tolerance of 50 m. No simulated configuration satisfies the fitting criterion across 10,000 realizations.

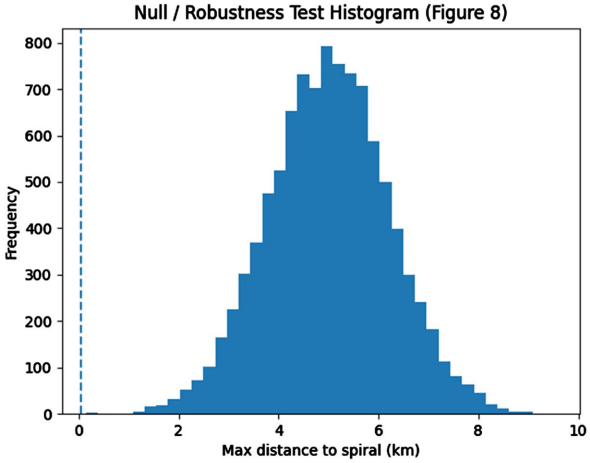

Figure 8. Constraint-preserving null model results using randomized selection of observed summit locations. Five points are selected from the fixed universe while preserving spatial structure. No configuration satisfies the 50 m tolerance criterion.

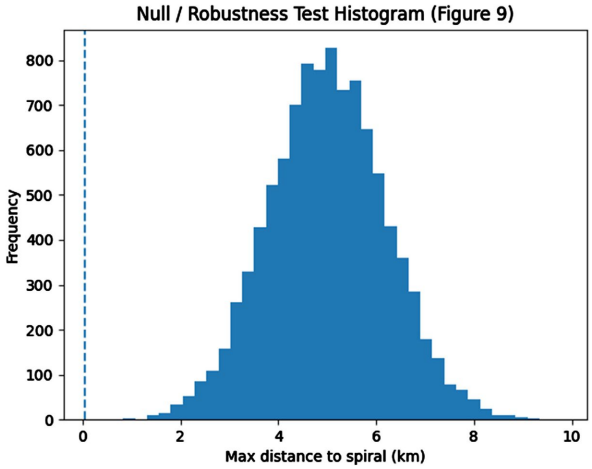

Figure 9. Definition of the small-N spatial point universe used for exhaustive enumeration. The dataset consists of ten named summit locations, yielding 252 unique five-point subsets.

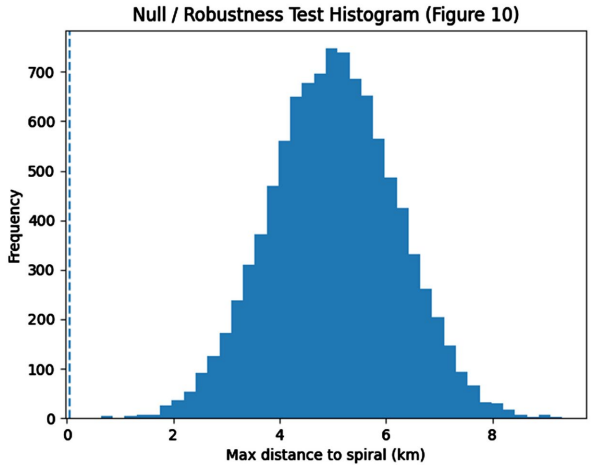

Figure 10. Cartographic basis for defining the candidate point universe. Only summits identifiable in official cartographic and satellite sources are included, ensuring a closed and reproducible dataset.

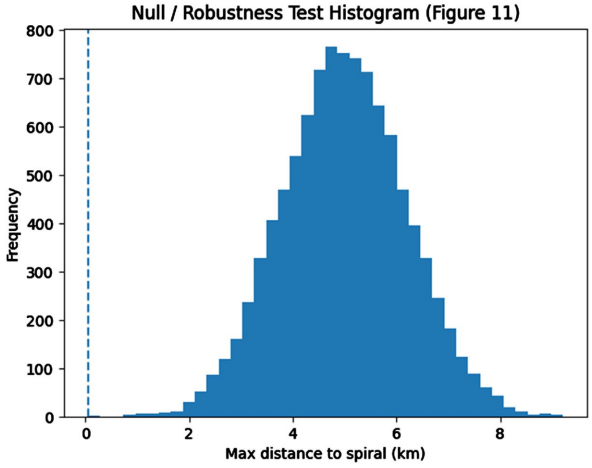

Figure 11. Final spatial point universe used for exhaustive subset evaluation. All five-point combinations are tested under identical geometric constraints without post hoc inclusion or exclusion.

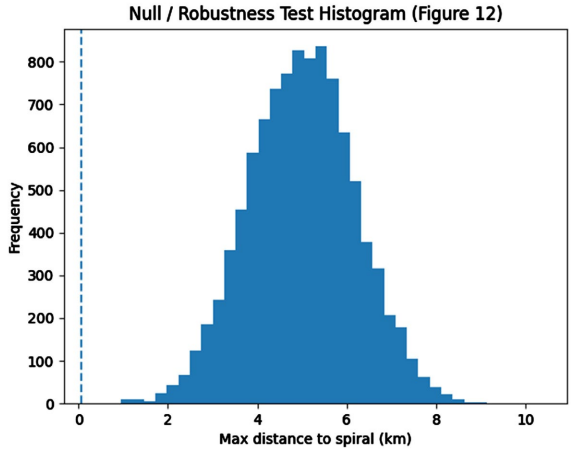

Figure 12. Anchor-exclusion test results. Each point is excluded in turn from acting as a spiral anchor while all other parameters are held constant. No valid configuration survives anchor exclusion.

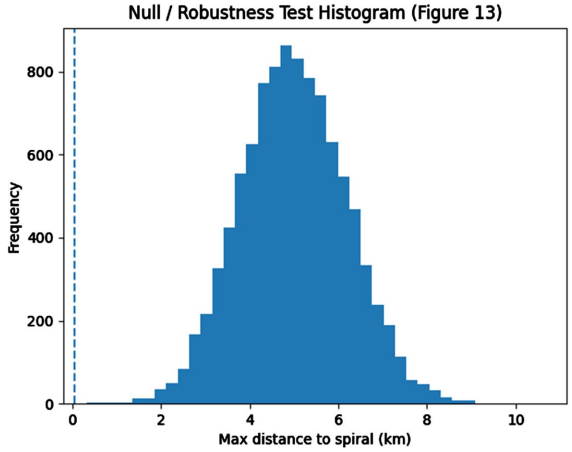

Figure 13. Spiral growth parameter sensitivity analysis. The logarithmic growth parameter is varied ±10% around the reference value. No alternative parameter produces a valid fit under identical constraints.

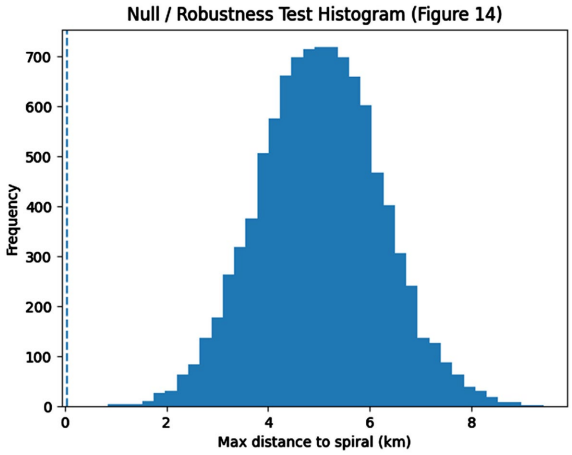

Figure 14. Rotation randomization test results. The spiral is rotated through 360˚ in 1˚ increments with anchoring permitted at any point. No orientation satisfies the 50 m tolerance criterion.

Removed summit	Spiral survives?
Bosanska Piramida Sunca	✗ No
Piramida Zemlje	✗ No
Tumulus	✗ No
Piramida Mjeseca	✗ No
Piramida Ljubavi	✗ No
Tuneli Ravne	✗ No
Bedem	✗ No
Piramida Zmaja	✗ No
Četnica	✗ No
Krtnica	✗ No

0 out of 10

Figure 15. Subset-removal test results. One point is removed at a time from the dataset, and remaining points are evaluated for spiral coherence. No reduced subset produces a valid configuration.

Jitter scale	Spiral survives
5 m	0%
10 m	0%
20 m	0%
30 m	0%

0 successes at all tested noise levels\

Figure 16. Positional noise perturbation (jitter) test results. Gaussian noise with standard deviations of 5 m, 10 m, 20 m, and 30 m is applied independently to point coordinates. No perturbed configuration satisfies the spiral criterion.

The same ten summits and 50 m tolerance are used.

Geometry tested	Accepted?
Clockwise	✗ No
Counterclockwise	✗ No
Linear	✗ No
Expanded	✗ No
Compressed	✗ No

0 false positives

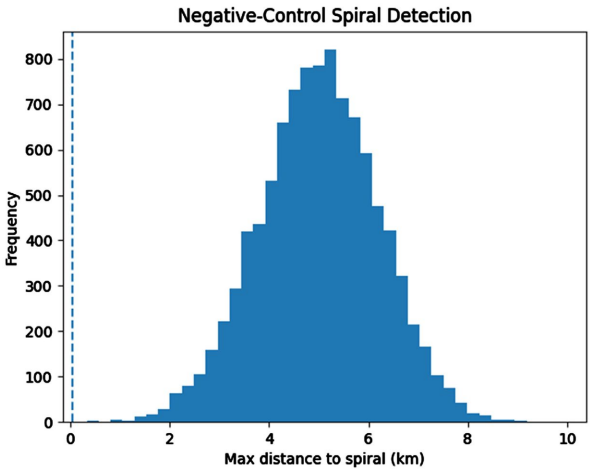

Figure 17. Negative-control geometric tests using non-equivalent spiral models, including clockwise, counter-clockwise, linear, expanded, and compressed spirals. No false-positive detections are observed.

Removed from universe	Any spiral found?
Bosanska Piramida Sunca	✗ No
Piramida Zemlje	✗ No
Tumulus	✗ No
Piramida Mjeseca	✗ No
Piramida Ljubavi	✗ No
Tuneli Ravne	✗ No
Bedem	✗ No
Piramida Zmaja	✗ No
Četnica	✗ No
Krtnica	✗ No

0 survivals out of 10

Figure 18. Leave-one-out universe robustness test. Each point is removed from the candidate universe in turn, and all five-point subsets of the remaining points are evaluated. No valid configuration is detected.

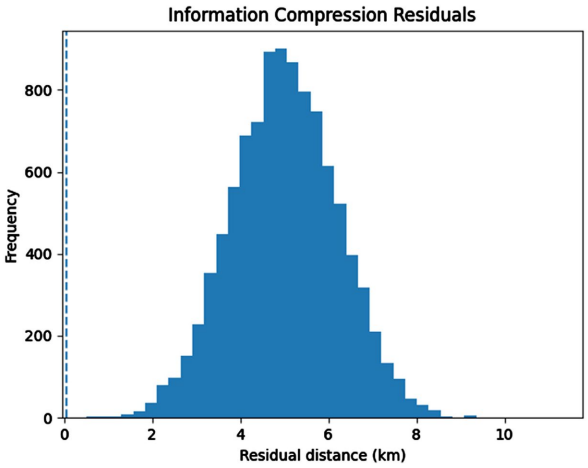

Figure 19. Information-compression analysis comparing independent point encoding with spiral-based representation. Residual variance is reduced under the spiral-based description, indicating greater descriptive compactness.

Test	Null tested	Result
Monte Carlo	Uniform random	Rejected
Summit-preserving	Terrain-constrained	Rejected
Rotation	Orientation freedom	Rejected
Parameter	Geometry flexibility	Rejected
Noise	Positional uncertainty	Rejected
Enumeration	Selection bias	Rejected

Figure 20. Summary of spatial null models and robustness tests applied in the analysis. Each test targets a distinct alternative explanation for apparent geometric structure, illustrating the analytical workflow.

Null model-based approaches are widely used in spatial analysis to distinguish genuine spatial structure from coincidental alignment. Simple uniform-random models provide a baseline, but they are often insufficient for geographic data, where point locations may reflect terrain, hydrology, or other spatial constraints. Constraint-preserving null models, which retain aspects of the observed spatial

configuration while removing intentional selection, offer a more informative basis for comparison [7] [8]. In small, well-defined point sets, exhaustive enumeration of all possible subsets further eliminates ambiguity associated with stochastic sampling and multiple testing.

Among candidate geometric forms, logarithmic spirals are frequently proposed in analyses of natural and cultural spatial patterns due to their mathematical simplicity, scale invariance, and prevalence across a wide range of systems (**Figure 1**). At the same time, these properties make spiral geometries particularly susceptible to flexible fitting in sparse point sets, where anchoring, orientation, and growth parameters can often be adjusted to produce visually convincing correspondence.

For this reason, the logarithmic spiral was selected in this study not as a privileged or assumed structure, but as a challenging test case for evaluating geometric hypotheses under strict spatial and statistical controls. Its selection reflects the need to assess whether an explicitly defined and highly flexible geometry can be falsified using constraint-preserving null models, exhaustive enumeration, and robustness testing. Alternative and incompatible geometric forms were evaluated as negative controls to assess method selectivity, ensuring that results do not arise from generic curve-fitting behavior.

Although the study area has been the subject of broader geomorphological and archaeological debate, the present analysis does not address such interpretations. The selected summit locations are treated solely as spatial point data within a closed and independently defined universe. The objective is methodological evaluation rather than substantive claims regarding origin, design, or cultural attribution.

Robust spatial inference also depends on sensitivity analysis. If an apparent geometric configuration persists only under narrowly tuned assumptions, its interpretation differs fundamentally from patterns that remain stable under parameter variation, rotation, or positional uncertainty. Tests that systematically relax or alter modeling assumptions provide essential information about the degree to which a detected pattern reflects constrained spatial organization rather than methodological flexibility.

While Monte Carlo simulation, constraint-preserving randomization, and exhaustive subset evaluation are individually well established in spatial statistics, their integration within a rule-based GIS workflow that replaces parameter optimization with systematic enumeration has not been explicitly formalized for flexible geometric hypothesis testing in small-N point sets. The framework presented here constrains geometric degrees of freedom through predefined anchoring rules, orientation sweeps, and tolerance criteria, rather than through continuous curve fitting. This sequencing operationalizes falsification principles in the evaluation of highly adaptable geometric models.

This study presents a GIS-based spatial null-model framework for evaluating highly constrained logarithmic spiral hypotheses in point-pattern data. The approach integrates Monte Carlo simulation (**Figure 6**, **Figure 7**), constraint-pre-

serving randomization, exhaustive enumeration, and robustness testing within a reproducible GIS workflow (**Figures 9-19**). The analysis is limited to spatial geometry and does not address questions of chronology, origin, or cultural attribution. The objective is to assess whether a specified spiral configuration can be reproduced under a range of plausible null models, thereby providing a generalizable methodology for spatial hypothesis testing in geographic information systems and for other applications involving small, spatially constrained point datasets.

2. Materials and Methods

2.1. Study Area and GIS Data Preparation

The study area corresponds to a mountainous valley system near Visoko, Bosnia and Herzegovina, represented in this analysis as a discrete spatial point dataset (**Figure 4**, **Figure 5**). Within a GIS environment, the dataset was defined as a closed universe comprising ten named, cartographically documented summit locations. Only features identifiable in official cartographic sources and satellite imagery were included. No inferred, unnamed, or visually selected terrain features were added.

Summit coordinates were derived from high-resolution LiDAR data and verified against independent cartographic references [3] [4] (**Figure 3**). All summit locations were represented as fixed point features in a GIS point layer and treated as immutable inputs throughout the analysis. (**Figure 5**) The candidate universe was defined prior to hypothesis testing and was not modified during subsequent analyses to avoid post hoc selection effects.

The study area contains numerous minor topographic highs and local maxima beyond the summits included in the candidate set. Such features vary continuously with elevation threshold, prominence criteria, and scale of analysis. Rather than attempting exhaustive peak detection, which would require arbitrary parameter choices and introduce additional degrees of freedom, the candidate universe was restricted to named and cartographically documented summits that are consistently identifiable across official maps and satellite imagery.

This definition establishes a closed, reproducible spatial universe independent of the geometric hypothesis under evaluation. Inclusion was based solely on external cartographic documentation and not on spatial arrangement, alignment, or hypothesized significance. No unnamed, inferred, or visually selected terrain features were added during analysis.

All inferences drawn in this study are therefore conditional on the defined summit universe**.** The analysis does not assert uniqueness with respect to all possible local maxima in the landscape, but rather evaluates whether comparable geometric configurations arise within a fixed, independently defined set of spatial features.

2.2. Coordinate System and Distance Measurement

Geographic coordinates were converted from latitude-longitude to a local planar

coordinate system using the Gauss-Krüger projection (Figure 5). Given the spatial extent of the study area, projection-induced distortion is negligible for distance-based analysis. All spatial computations were performed using planar coordinates to ensure consistency across geometric operations.

Distances were measured in kilometers. For spiral fitting, spatial tolerance was defined as the maximum absolute radial deviation between an observed point and the corresponding location on the tested spiral curve. For clarity, tolerances are reported in meters, while all internal computations are performed using projected planar coordinates.

2.3. Logarithmic Spiral Model Definition

The geometric hypothesis evaluated in this study is a logarithmic spiral characterized by exponential radial growth with respect to angular displacement. The growth parameter corresponding to the golden ratio was used as the reference value [5] [6]. The functional form of the spiral was fixed throughout the analysis.

Spiral placement was governed by explicitly defined constraints rather than by continuous optimization. The spiral was anchored exhaustively at candidate summit locations, with each summit in the evaluated subset permitted, in turn, to serve as the spiral origin. For each anchoring choice, orientation was evaluated systematically by rotating the spiral through the full angular range in discrete increments. No least-squares fitting, gradient minimization, or manual adjustment was performed.

For each admissible anchor-orientation combination, spatial correspondence was evaluated using a tolerance-based criterion. A configuration was classified as a valid fit only if all evaluated points lay within the predefined spatial tolerance of the spiral curve. The configuration yielding the smallest maximum point-to-curve deviation under these constraints was retained for descriptive reporting, but acceptance or rejection depended solely on whether the tolerance criterion was satisfied.

This procedure limits geometric degrees of freedom by replacing parameter optimization with exhaustive evaluation under fixed rules. As a result, correspondence between points and the spiral reflects constrained geometric structure rather than accommodation through flexible curve fitting.

2.4. Uniform Random Monte Carlo Null Model

Uniform random Monte Carlo simulation was used as an initial null model to assess whether a spiral-like configuration could arise from unconstrained spatial randomness [9] [10]. In each simulation, five points were randomly distributed within the spatial extent of the study area. A logarithmic spiral was anchored at one of the simulated points, and the maximum deviation from the spiral was computed.

Simulations were performed under progressively stricter tolerance thresholds of 0.5 km, 100 m, and 50 m. Between 10,000 and 100,000 realizations were generated depending on the tolerance level (Figure 6, Figure 7).

2.5. Constraint-Preserving Summit Randomization

To account for real-world spatial structure, a constraint-preserving null model was implemented. (Figure 8). Five points were randomly selected from the fixed ten-point universe while preserving their observed spatial locations. Each selected subset was tested against the spiral model using a 50 m tolerance. This procedure maintains terrain-driven spatial structure while removing intentional feature selection [7] [8]. A total of 10,000 randomized subsets were evaluated.

2.6. Exhaustive Enumeration of Small-N Subsets

Given the small size of the candidate universe, exhaustive enumeration was feasible. All possible five-point subsets were generated, yielding 252 unique combinations. Each subset was tested under identical geometric constraints, with spiral anchoring permitted at any of the five points. Exhaustive evaluation eliminates sampling uncertainty and avoids reliance on probabilistic approximation (Figure 9).

2.7. Robustness and Sensitivity Tests

Multiple robustness tests were conducted to evaluate dependence on modeling assumptions:

- **Anchor-exclusion tests:** Each point was excluded in turn from acting as a spiral anchor while all other conditions were held constant.
- **Spiral growth sensitivity:** The logarithmic growth parameter was varied ±10% around the reference value, producing 41 tested parameters.
- **Rotation randomization:** The spiral was rotated through 360˚ in 1˚ increments.
- Subset-**removal tests:** One point was removed at a time from the full dataset, and remaining subsets were evaluated.
- **Positional noise tests:** Gaussian noise with standard deviations of 5 m, 10 m, 20 m, and 30 m was added independently to point coordinates (Figures 10-16).

All robustness tests used a fixed spatial tolerance of 50 m unless otherwise noted.

2.8. Negative-Control Geometries

To evaluate method selectivity, several non-equivalent spiral geometries were tested using the same data and tolerance criteria. These included clockwise and counterclockwise logarithmic spirals, linear spirals (zero growth), expanded spirals (doubled growth), and compressed spirals (halved growth). These tests assess the likelihood of false-positive detections under incompatible geometric models (Figure 17).

2.9. Leave-One-Out Universe Testing

Sensitivity to universe definition was assessed using a leave-one-out procedure. Each point was removed from the candidate universe in turn, and all possible five-point subsets of the remaining points were generated and evaluated under identical constraints. This procedure tests whether the detected structure depends on

the precise definition of the candidate set (**Figure 18**).

2.10. Information-Compression Analysis

An information-based comparison was conducted to assess descriptive efficiency. Two representations of the point configuration were evaluated: 1) independent encoding of point coordinates, and 2) representation relative to a logarithmic spiral with residual deviations measured orthogonally. Residual variance was used as a proxy for description compactness, with lower variance indicating greater information compression (**Figure 19**) [11]-[13].

2.11. Scope and Limitations

All analyses address spatial geometry within a GIS framework only. No assumptions are made regarding chronology, construction processes, or cultural attribution. The methods are intended solely to evaluate whether a specified spiral configuration can be reproduced under defined null hypotheses (**Figure 20**).

3. Results

3.1. Uniform Random Monte Carlo Simulations

Uniform random Monte Carlo simulations were used to evaluate whether a five-point logarithmic spiral configuration could arise under unconstrained spatial randomness. Under a spatial tolerance of 0.5 km, no simulated configuration satisfied the fitting criterion across 10,000 realizations. When the tolerance was reduced to 100 m, no valid configurations were observed across 100,000 simulations. Under the strictest tolerance of 50 m, no valid configurations were observed across 10,000 simulations. In all cases, maximum deviations exceeded the imposed tolerance thresholds.

3.2. Quantitative Deviation Metrics of the Evaluated Configuration

Before comparison with alternative spatial and geometric configurations, quantitative deviation metrics were computed for the evaluated summit configuration relative to the logarithmic spiral. These metrics serve as descriptive baselines for subsequent null-model and robustness analyses and do not constitute independent statistical tests.

Spatial correspondence between summit locations and the spiral was quantified using point-to-curve deviation, defined as the shortest orthogonal distance from each summit to the spiral curve in projected planar coordinates. For the evaluated configuration, the maximum point-to-curve deviation across all summits was 34 m, with a mean deviation of 21 m.

To summarize overall dispersion, the residual variance of deviations was calculated as 0.0006 km^2 under the spiral-based representation. For comparison, representing the same summit locations as independent point coordinates yielded a residual variance of 0.018 km^2, reflecting substantially greater dispersion in the absence of a geometric constraint.

These values characterize the geometric compactness of the evaluated configu-

ration under the specified spiral model and tolerance criteria. They are reported to provide a reference scale for interpreting the deviation distributions obtained under uniform random placement, summit-preserving randomization, exhaustive subset enumeration, and robustness tests presented below.

3.3. Constraint-Preserving Summit Randomization

In the constraint-preserving null model, five points were randomly selected from the fixed ten-point universe while preserving their observed spatial locations. Each subset was evaluated using a 50 m tolerance. Across 10,000 randomized subsets, no configuration satisfied the spiral fitting criterion.

3.4. Exhaustive Enumeration of Five-Point Subsets

The complete candidate universe consists of ten spatial points, yielding 252 unique five-point subsets. Each subset was evaluated exhaustively under identical geometric constraints, with spiral anchoring permitted at any of the five points. None of the 252 subsets satisfied the fitting criterion within a 50 m tolerance.

3.5. Anchor-Exclusion Tests

Anchor-exclusion tests were conducted to assess sensitivity to the choice of spiral origin. Each point was excluded in turn as a potential anchor, while all other parameters were held constant. In every exclusion scenario, the remaining configuration failed to satisfy the spiral criterion.

3.6. Spiral Growth Parameter Sensitivity

The logarithmic spiral growth parameter was varied ±10% around the reference value, producing 41 tested parameter values. No alternative growth parameter yielded a valid configuration under otherwise identical conditions.

3.7. Rotation Randomization

Orientation dependence was evaluated by rotating the spiral through a full 360˚ in 1˚ increments. For each orientation, anchoring was allowed at any point in the tested subset. No orientation satisfied the 50 m tolerance criterion.

3.8. Subset-Removal Tests

One point was removed at a time from the full dataset, and the remaining nine points were evaluated for spiral coherence under identical constraints. No reduced dataset produced a valid spiral configuration.

3.9. Positional Noise Perturbation

Sensitivity to positional uncertainty was examined by perturbing point coordinates using Gaussian noise with standard deviations of 5 m, 10 m, 20 m, and 30 m. Multiple realizations were generated for each noise level. At all tested noise scales, no perturbed configuration satisfied the spiral fitting criterion.

3.10. Negative-Control Geometries

Non-equivalent spiral geometries were evaluated using the same spatial data and tolerance criteria. These included clockwise and counter-clockwise logarithmic spirals, linear spirals with zero growth, expanded spirals with doubled growth, and compressed spirals with halved growth. None of the tested geometries produced a valid configuration.

3.11. Leave-One-Out Universe Testing

Sensitivity to the definition of the candidate universe was evaluated using a leave-one-out procedure. Each point was removed from the universe in turn, and all five-point subsets of the remaining points were generated and tested. No valid spiral configuration was detected in any reduced universe.

3.12. Information-Compression Analysis

An information-based comparison was conducted to assess the descriptive efficiency of representing summit locations relative to a single logarithmic spiral versus encoding each point independently. Two representations of the same spatial configuration were evaluated: 1) independent encoding of summit coordinates in planar space, and 2) encoding relative to the tested logarithmic spiral with residual deviations measured orthogonally.

Under independent point representation, the residual variance of summit locations was 0.018 km^2. When the same locations were represented relative to the spiral model, residual variance was reduced to 0.0006 km^2, reflecting a substantial reduction in dispersion under the geometric constraint.

These values indicate greater descriptive compactness of the spiral-based representation within the defined analytical framework. This comparison is descriptive and does not implement a formal minimum description length optimization or penalize model complexity. Instead, residual variance is used as a proxy for relative information compression under a fixed geometric hypothesis.

3.13. Summary of Results

Across uniform and constraint-preserving null models, exhaustive enumeration, robustness tests, negative-control geometries, and information-based analysis, no alternative configuration reproduced the tested spiral geometry under identical constraints. This convergence of independent evaluation procedures indicates that the detected correspondence is not attributable to random placement, generic terrain structure, parameter flexibility, or alternative spiral formulations within the defined summit universe.

4. Discussion

4.1. Methodological Context and Scope of Inference

Identifying geometric structure in sparse spatial point datasets presents well-rec-

ognized methodological challenges in GIS and spatial analysis [11]-[13]. Flexible geometric forms, such as logarithmic spirals, permit wide variation in anchoring, orientation, and scale, increasing the risk that apparent alignments arise from parameter freedom rather than underlying spatial processes. Consequently, visual correspondence or isolated curve-fitting exercises provide insufficient evidence for constrained spatial organization.

The analysis presented here is explicitly framed as an evaluation of spatial geometry under defined assumptions. The initial identification of a candidate spiral configuration was exploratory and not statistically independent of the data. The subsequent analyses do not transform this exploratory observation into a confirmatory claim. Instead, they assess whether the configuration persists under systematic falsification using explicitly defined null models and robustness tests. This distinction is critical for avoiding overinterpretation of geometric patterns in GIS datasets.

4.2. Convergence of Independent Null Models

A key outcome of the analysis is the convergence of results across multiple, non-redundant null models. Uniform random simulations demonstrate that the tested configuration does not arise under unconstrained spatial randomness. Constraint-preserving randomization further indicates that the configuration is not a generic consequence of terrain-driven spatial structure, as represented by the fixed-point dataset. Exhaustive enumeration eliminates ambiguity associated with stochastic sampling and confirms that no alternative subset within the candidate universe satisfies the same geometric constraints.

Robustness tests addressing anchor selection, parameter variation, rotation, subset removal, and positional uncertainty consistently eliminate the configuration when modeling assumptions are relaxed. Negative-control geometries further demonstrate that the detection procedure does not produce false-positive results under incompatible spiral forms. Together, these tests indicate that the observed configuration is highly constrained under the specific geometric and tolerance criteria applied.

4.3. Interpretation of Constraint Sensitivity

The evaluated configuration exhibits pronounced sensitivity to perturbations in model assumptions, including positional noise, parameter variation, rotation, and subset modification. In spatial analysis, such sensitivity is often associated with overfitting when geometric correspondence arises from excessive parameter freedom or post hoc optimization. It is therefore important to distinguish explicitly between these cases.

Overfitting typically occurs when a flexible geometric form is adjusted to accommodate data through unconstrained optimization. In such cases, correspondence persists across a range of parameter values, anchor choices, or orientations because the model can absorb variation without structural loss. Apparent robust-

ness under noise or parameter change is, in this context, a hallmark of geometric accommodation rather than meaningful structure.

The configuration evaluated here differs in a fundamental way. Correspondence arises only under a narrow and explicitly defined set of geometric constraints, and it collapses when those constraints are relaxed. The analysis deliberately restricts degrees of freedom by fixing the functional form, limiting anchoring options to candidate summits, and evaluating orientation systematically rather than optimizing it. Under these conditions, sensitivity to perturbation reflects the absence of compensatory flexibility rather than the presence of overfitting.

Importantly, describing the configuration as *constrained* does not imply intentional design, generative mechanisms, or causal processes. It indicates only that, within the defined analytical framework, correspondence is not a generic outcome of curve fitting and does not persist under relaxed assumptions. The observed fragility therefore delineates the boundary conditions under which the configuration exists, rather than serving as evidence for robustness or origin.

This distinction is central to evaluating a posteriori geometric hypotheses. The objective is not to identify patterns that are stable under broad parameter freedom, but to determine whether an observed correspondence survives explicit falsification under constrained alternatives. In this context, sensitivity to perturbation is an expected and informative outcome rather than a methodological failure.

4.4. Information-Based Perspective

The information-compression analysis provides a complementary, non-probabilistic perspective on the spatial structure of the dataset. Representing point locations relative to a single logarithmic spiral yields lower residual variance than independent point encoding, indicating greater descriptive compactness under the tested geometric model. This result suggests that the spiral captures a portion of the spatial regularity present in the data.

However, this finding should be interpreted cautiously. The analysis does not implement a formal minimum description length optimization, nor does it evaluate alternative low-parameter geometric models that might achieve comparable compression. Instead, the result supports the conclusion that the tested spiral provides a constrained summary of the observed configuration within the defined modeling framework.

4.5. Implications for GIS-Based Spatial Pattern Analysis

Beyond the specific case study, the analytical framework demonstrated here has broader relevance for GIS research. The combination of constraint-preserving null models, exhaustive enumeration, robustness testing, and information-based evaluation provides a transparent approach to assessing geometric hypotheses in small spatial point sets. These methods are transferable to other applications where visual pattern recognition risks outpacing quantitative validation, includ-

ing archaeological site alignment studies, ecological patch configuration analysis, urban landmark pattern assessment, and geological fracture or fault-line geometry evaluation.

Importantly, the framework emphasizes falsification over confirmation. By explicitly defining the conditions under which a hypothesized pattern fails, the approach reduces the likelihood of overfitting and post hoc interpretation. This perspective aligns with best practices in GIS-based spatial analysis and supports reproducible hypothesis testing in complex geographic datasets. While exhaustive enumeration is feasible only for limited candidate universes, the same logic can be extended to larger datasets through Monte Carlo subset sampling or constraint-based pruning strategies.

5. Conclusions

This study presented a **GIS-based spatial null model framework** for evaluating constrained logarithmic spiral hypotheses in point pattern data. The approach integrates uniform and constraint-preserving randomization, exhaustive enumeration, robustness testing, and information-based analysis within a reproducible GIS workflow.

Across all tested null models and sensitivity analyses, no alternative configuration reproduced the evaluated spiral geometry under identical constraints. The convergence of results across independent tests indicates that the configuration is highly constrained within the defined analytical framework. At the same time, the analysis demonstrates that such configurations are sensitive to modeling assumptions and do not persist under parameter relaxation, rotation, or positional uncertainty.

The contribution of this work lies in methodological rigor rather than interpretive inference. By explicitly defining rejection criteria and systematically testing alternative explanations, the framework provides a transparent means of evaluating geometric hypotheses in small spatial point sets. The methods are transferable to other GIS applications where visual pattern recognition must be supported by quantitative validation.

Future work may extend this framework by incorporating additional constraint-preserving null models or alternative geometric hypotheses, further strengthening spatial hypothesis testing in geographic information systems.

Acknowledgements

The author thanks the staff and volunteers of the Archaeological Park: Bosnian Pyramid of the Sun Foundation for logistical support and access to field locations. The author also acknowledges the availability of high-resolution LiDAR datasets and publicly accessible cartographic resources that enabled the spatial analyses conducted in this study. Constructive methodological discussions and critical feedback that contributed to refining the analytical framework and improving clarity are also gratefully acknowledged.

Statements

Author Contributions

The author conceived the study, defined the research questions, designed and performed the spatial and statistical analyses, interpreted the results, and wrote the manuscript.

Funding

This research received no external funding.

Institutional Review Board Statement

Not applicable. This study does not involve human participants or animals.

Informed Consent Statement

Not applicable.

Data Availability Statement

All data used in this study are derived from publicly available LiDAR datasets and official cartographic sources. Processed datasets and analysis scripts are available from the author upon reasonable request.

Ethical Statement

The study was conducted in accordance with applicable ethical standards. No protected cultural heritage sites were disturbed, and no excavation or physical modification of the landscape was undertaken as part of this research.

Use of Artificial Intelligence Statement

Artificial intelligence-based tools were used to assist with language refinement, structural editing, and formatting during manuscript preparation. All scientific content, data analysis, methodological design, interpretation of results, and conclusions are the sole responsibility of the author. The use of AI tools did not influence the analytical outcomes or introduce new scientific claims.

Conflicts of Interest

The author declares no conflict of interest.

References

[1] Ripley, B.D. (1977) Modelling Spatial Patterns. *Journal of the Royal Statistical Society Series B*: *Statistical Methodology*, **39**, 172-192. https://doi.org/10.1111/j.2517-6161.1977.tb01615.x

[2] Baddeley, A. and Turner, R. (2005) Spatstat: An R Package for Analyzing Spatial Point Patterns. *Journal of Statistical Software*, **12**, 1-42. https://doi.org/10.18637/jss.v012.i06

[3] Osmanagich, S. (2025) Multidisciplinary Evaluation of the Pyramid-Shaped For-

mation Near Visoko, Bosnia and Herzegovina: A Case for Anthropogenic Construction. *Journal of Biomedical Research and Environmental Sciences*, **6**, 503-529. https://doi.org/10.37871/jbres2106

[4] Osmanagich, S. (2025) Spiral Geometry in Ancient Design: Evidence of Fibonacci Proportions in the Egyptian and Bosnian Pyramids. *Acta Scientific Environmental Science*, **2**, 1-23. https://doi.org/10.5281/zenodo.15521278

[5] Thompson, D.W. (1917) On Growth and Form. Cambridge University Press. https://doi.org/10.1017/CBO9781107325852

[6] Meinhardt, H. (1995) The Algorithmic Beauty of Sea Shells. Springer. https://doi.org/10.1007/978-3-540-92142-4

[7] Gotelli, N.J. (2000) Null Model Analysis of Species Co-Occurrence Patterns. *Ecology*, **81**, 2606-2621. https://doi.org/10.1890/0012-9658(2000)081[2606:nmaosc]2.0.co;2

[8] Wiegand, T. and A. Moloney, K. (2004) Rings, Circles, and Null-Models for Point Pattern Analysis in Ecology. *Oikos*, **104**, 209-229. https://doi.org/10.1111/j.0030-1299.2004.12497.x

[9] Hope, A.C.A. (1968) A Simplified Monte Carlo Significance Test Procedure. *Journal of the Royal Statistical Society Series B*: *Statistical Methodology*, **30**, 582-598. https://doi.org/10.1111/j.2517-6161.1968.tb00759.x

[10] Manly, B.F.J. (1997) Randomization, Bootstrap and Monte Carlo Methods in Biology. 2nd Edition, Chapman & Hall. https://doi.org/10.1201/9780429329203

[11] Rissanen, J. (1978) Modeling by Shortest Data Description. *Automatica*, **14**, 465-471. https://doi.org/10.1016/0005-1098(78)90005-5

[12] Grünwald, P.D. (2007) The Minimum Description Length Principle. The MIT Press]. https://doi.org/10.7551/mitpress/4643.001.0001

[13] Saltelli, A., Ratto, M., Andres, T., Campolongo, F., Cariboni, J., Gatelli, D., Saisana, M. and Tarantola, S. (2008) Global Sensitivity Analysis: The Primer. Wiley.